Development of a Nano-Impulse Balance for Micropropulsion Systems

Brian C. D'Souza
University of Southern California, Dept. of Aerospace and Mechanical Engineering, Los Angeles, CA 90089-1191

and

Andrew D. Ketsdever
US Air Force Academy, Dept. of Astronautics, Colorado Springs, CO 80840

Several versions of a torsional impulse balance have been developed as a new diagnostic tool to study fundamental physical processes in micropropulsion systems. With respect to the transfer of momentum, direct measurements of the transient forces or total impulse delivered can lead to a better understanding and characterization of the efficiency of the thrust that is possible under different configurations. The impulse balance has been designed and tested with a robust calibration system to measure steady state and impulsive forces. The behavior of the impulse balance was thoroughly studied and characterized. An analytical model of the balance's motion was developed from the general equation of motion of an underdamped, harmonically oscillating system. A simple technique has been developed to accurately back out the force as a function of time from the experimental data. The latest version of the impulse balance also manages to resolve changes in mass, which is another key parameter of propulsion efficiency. These impulse balances have been used in different configurations to study many forms of micropropulsion, including the impulses caused by laser-surface interactions and the combustion of Tanner Research, Inc. MEMS-based solid-propellant motors.

Nomenclature

α	=	damping term in equations of motion (sec^{-1})
β	=	frequency term in equations of motion (sec^{-1})
δ	=	damping ratio, $\ln[x_{max1}/x_{max2}]$
$\mathcal{I}$	=	impulse, $\int F(t)dt$ (N·sec)
τ	=	pulsewidth (sec)
θ	=	angular displacement or deflection (rad)
$\dot{\theta}$	=	angular velocity (rad/sec)
$\ddot{\theta}$	=	angular acceleration (rad/sec^2)
ω_n	=	natural (angular) frequency (sec^{-1})
C	=	viscous damping coefficient ($kg \cdot m^2/sec$)
F	=	force (N)
I	=	moment of inertia ($kg \cdot m^2$)
K	=	spring constant (N/m)
M	=	moment or torque, F · r (N·m)
r	=	moment arm (m)
T	=	period (sec)
t	=	time (sec)
x	=	linear displacement or deflection (m)
$\dot{x}$ or v	=	linear velocity (m/sec)
$\ddot{x}$ or a	=	linear acceleration (m/sec^2)

Report Documentation Page

Form Approved
OMB No. 0704-0188

1. REPORT DATE	2. REPORT TYPE	3. DATES COVERED
JUN 2005		**-**

4. TITLE AND SUBTITLE	5a. CONTRACT NUMBER
Development of a Nano-Impulse Balance for Micropropulsion Systems	5b. GRANT NUMBER
	5c. PROGRAM ELEMENT NUMBER
6. AUTHOR(S)	5d. PROJECT NUMBER
Brian D'Souza; Andrew Ketsdever	**5026**
	5e. TASK NUMBER **0568**
	5f. WORK UNIT NUMBER
7. PERFORMING ORGANIZATION NAME(S) AND ADDRESS(ES)	8. PERFORMING ORGANIZATION REPORT NUMBER
Air Force Research Laboratory (AFMC),AFRL/PRSA,10 E. Saturn Blvd.,Edwards AFB,CA,93524-7680	
9. SPONSORING/MONITORING AGENCY NAME(S) AND ADDRESS(ES)	10. SPONSOR/MONITOR'S ACRONYM(S)
	11. SPONSOR/MONITOR'S REPORT NUMBER(S)

12. DISTRIBUTION/AVAILABILITY STATEMENT

Approved for public release; distribution unlimited

13. SUPPLEMENTARY NOTES

14. ABSTRACT

Several versions of a torsional impulse balance have been developed as a new diagnostic tool to study fundamental physical processes in micropropulsion systems. With respect to the transfer of momentum, direct measurements of the transient forces or total impulse delivered can lead to a better understanding and characterization of the efficiency of the thrust that is possible under different configurations. The impulse balance has been designed and tested with a robust calibration system to measure steady state and impulsive forces. The behavior of the impulse balance was thoroughly studied and characterized. An analytical model of the balance's motion was developed from the general equation of motion of an underdamped, harmonically oscillating system. A simple technique has been developed to accurately back out the force as a function of time from the experimental data. The latest version of the impulse balance also manages to resolve changes in mass, which is another key parameter of propulsion efficiency. These impulse balances have been used in different configurations to study many forms of micropropulsion, including the impulses caused by laser-surface interactions and the combustion of Tanner Research, Inc. MEMS-based solidpropellant motors.

15. SUBJECT TERMS

16. SECURITY CLASSIFICATION OF:			17. LIMITATION OF ABSTRACT	18. NUMBER OF PAGES	19a. NAME OF RESPONSIBLE PERSON
a. REPORT	b. ABSTRACT	c. THIS PAGE			
unclassified	**unclassified**	**unclassified**		**12**	

I. Introduction

There are a number of applications of current interest where the knowledge of time resolved forces would be beneficial to the basic understanding of physical processes. For spacecraft propulsion, fine attitude control requires precise and reproducible impulse delivery from the thruster system. Although total delivered impulse is generally measured and deemed adequate for most mission scenarios, time resolved thrust measurements would be beneficial in understanding the physics of thruster operation and could lead to the development of more precise and efficient thruster systems.

For example, pulsed plasma thrusters (PPT) use a spark generated across a Teflon propellant to produce an energetic arc-ablated ionized plume.[1] The total impulse delivery from a PPT involves a relatively low mass of highly energetic ions and a large mass of slow moving molecules and heavier particles as shown schematically in Fig. 1a. The initially ablated material produces the majority of the thrust. Subsequent heat adsorption by the Teflon produces a late-time ablative plume of relatively massive, slow moving molecules and particles.[2] The late-time ablation does not produce significant thrust; however, a relatively large amount of propellant mass is lost in this process leading to thruster inefficiencies. Although the total impulse, $\mathcal{I}$, obtained from integrating F(t) versus time in Fig. 1a and Fig. 1b are the same, the detailed physics behind the production of each impulse curve may be quite different.

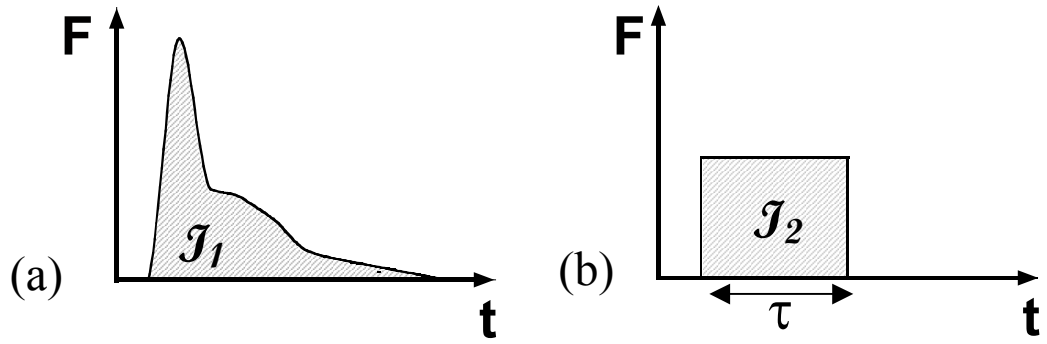

Figure 1. Schematic of two very different force profiles that result in equivalent total impulses $\mathcal{I}_1=\mathcal{I}_2$. (a) Large initial force with smaller residuals. (b) Constant force of pulsewidth t.

A simple analysis based on the total impulse would not yield any information about the pulse shape. The investigation of the time dependent forces produced by a PPT can lead to more efficient thrusters by investigating system changes that maximize the efficient production of ionized propellant and minimize the production of late-time ablation. A measure of propulsive efficiency is the specific impulse, I_{sp}, given by

$$I_{sp} = \frac{1}{M_p g_o} \int_{t=0}^{t=t'} F(t)dt \tag{1}$$

where F(t) is the time dependent force produced by the thruster, t' is the thruster's pulse duration, and M_p is the total mass of the propellant lost in the pulse, and g_o is the Earth's gravitational constant. From Eq. (1), it can be seen that details of the impulse delivery in the integral are important for thruster efficiency. With respect to the transfer of momentum, direct measurements of the transient forces can lead to a better understanding and characterization of the efficiency of the thrust that is possible under different configurations.

Many impulse balances have been designed to measure steady state and transient forces produced by a variety of processes.[3-5] Commonly, the impulse generated is investigated by measuring the maximum deflection of the balance caused by a given impulse.[4,5] There are two major shortcomings of this approach. First, there is no information that can be inferred from this data regarding the pulse width, τ, or the pulse shape. Second, it is only strictly valid for $\tau \ll T$. Since very different pulse widths and shapes can lead to the same maximum deflection on an impulse balance, the simple method of investigating a balance's maximum deflection is not always adequate to determining the characteristics of the impulse delivered. A detailed analysis of the impulse balance's equation of motion can lead to a more complete understanding of the complex physical processes which may be driving device operation.

Several versions of a simple torsional impulse balance have been developed as a diagnostic tool to study fundamental physical processes in micropropulsion systems. Early versions, such as the nano-Newton Thrust Stand (nNTS)[6], focused on steady state force measurements. An Electrostatic Force Calibration System (EFCS) using an electrostatic comb force calibration technique described by Selden and Ketsdever[7] has been employed to accurately calibrate the system to provide precise and repeatable measurements. Then, a uniquely successful nano-Newton-second impulse balance system (NIBS)[8] capable of resolving total impulse measurements as low as 7 nano-Newton-seconds (nNs) was designed and constructed. The EFCS evolved to provide a robust calibration scheme using both steady state and impulsive force delivery. The behavior of the NIBS was thoroughly studied and characterized. An analytical model of the balance's motion was developed from the general equation of motion of an underdamped, harmonically oscillating system. A simple technique has been developed to accurately back out the force as a function of time from the experimental data. The latest version of the impulse balance, referred to as the Thrust Stand micro-Mass Balance (TSMB)[9], manages to additionally resolve changes in mass, which is another key parameter of propulsion efficiency.

Currently, there are a number of research endeavors using versions of the NIBS to perform impulse measurements on fundamental laser-surface interactions and innovative propulsion devices. Some initial experiments have been conducted for laser ablation impulse measurements. These preliminary tests were done using a Nd:YAG laser at 532nm and 1064nm on various metal and polymer targets. Similarly, the TSMB is being used to study propulsion devices where change in mass due to propellant consumption is significant. Initial testing has been done using a set of experimental small solid-propellant motors in air. Minor modifications were made to the NIBS to handle a higher range of forces. But the calibration methods, and analysis techniques (both steady-state and impulsive) still prove to be valid and reliable.

This paper will focus primarily on the design of the impulse balances and the range of measurement techniques that can be used to provide a robust diagnostic tool. While results from testing of actual propulsion devices and other propulsive effects will be presented, the details of the thruster designs and physical principles involved will not be discussed in detail here.

II. Impulse Balance Systems

All of the balance systems are based upon a torsional thrust stand design.[6] As shown in Fig. 2, the NIBS is a torsional pendulum with viscous damping provided by an oil bath. Two flexure pivots provide the restoring force for the system. The entire structure is made of aluminum to keep the balance's moment of inertia as low as possible in an attempt to maximize the deflection for a given applied force. Propulsion systems or test materials are mounted at the end of the 45 cm long arms. The Electrostatics Force Calibration System (EFCS) is mounted on the end of one arm at the same location from the center of rotation as the impulse delivery is expected. The NIBS motion is sensed by a linear variable differential transducer (LVDT). The LVDT senses a linear motion at the end of the balance's arm, which can be transformed into a rotational deflection. The data trace obtained by monitoring the LVDT output over time provides the basis for deriving the impulse imparted to the NIBS. A damping cup is mounted to the bottom of the NIBS and is placed in an oil bath to provide viscous damping, which is essential for damping out the motion of the stand in vacuum.

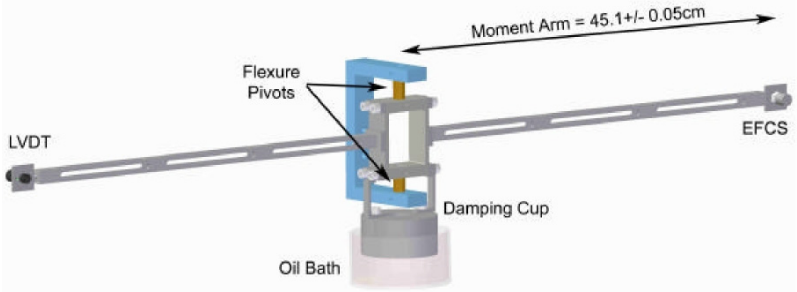

Figure 2. Schematic of the nano-Newton impulse balance system (NIBS).

The TSMB has been designed based on the nNTS[6] and NIBS[8] systems, which resolve thrust measurements from a torsion pendulum that pivots around a vertical axis of rotation. A force imparted to these stands results in a horizontal displacement of the target. The TSMB, as shown in Fig. 3, has evolved these designs by rotating the stand 90° to provide a horizontal axis of rotation. The TSMB system relies on precise mass and inertia balance of the symmetrical arms abut the pivot axis. Changes in mass are observed as a steady-state force resulting from the

imbalance of the system as propellant is exhausted. A number of other modifications have been made necessary by the change in geometry, such as the removal of the oil baths used to provide viscous damping on the stand. In its place, an electromagnetic damping system has been adopted to provide damping in a manner consistent with the viscous oil. In addition, the electromagnetic damping system will help to mitigate the contamination potential of viscous oil.

The impulse balances have been made to operate in a wide range of ambient environments. Testing has

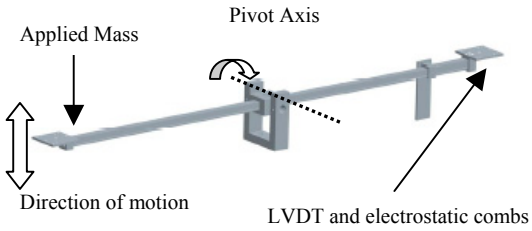

Figure 3. Schematic of the Thrust Stand micro-Mass Balance (TSMB).

successfully been performed in many gases at a range of pressures from 1atm down to 10^{-6} Torr. In the presence of gases, the impulse balances can be calibrated to account for any additional damping forces. However, care must be taken to minimize random air currents, as the impulse balances are very sensitive. So all tests must be conducted in a sealed vacuum chamber or some other form of enclosure. Figure 4 depicts a typical setup for an impulse balance.

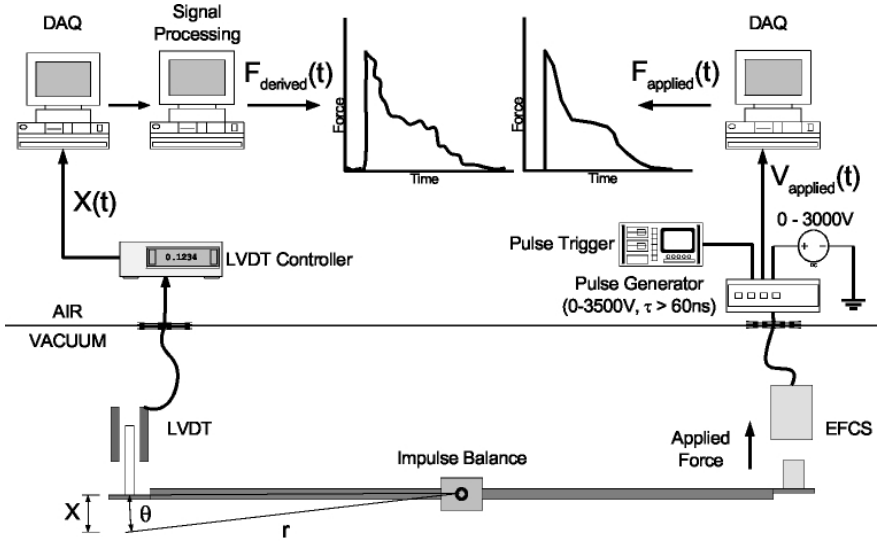

Figure 4. Schematic of typical experimental setup and process for obtaining the derived and applied forces imparted to the impulse balance as a function of time.

For calibration of the system, impulse delivery to the NIBS is accomplished by supplying a potential difference to the Electrostatic Force Calibration System (EFCS). The EFCS consisted of an aluminum comb assembly[7] with one side of the EFCS assembly attached directly to the NIBS. As shown in the experimental setup in Figure 4, the power supply for the EFCS is attached to a pulse generator capable of delivering ±3500 V with a 20 ns rise time and a variable DC pulse width (minimum of 60 ns). The output of the pulse generator is sent directly to the EFCS assembly in the chamber through a high voltage vacuum feed-through and is monitored by the 18-bit data acquisition (DAQ) system. The applied (and monitored) voltage to the EFCS is used to calculate the actual impulse applied to the NIBS. Calibration of the NIBS is a critical element of this study. Through repeated calibration tests in the actual experimental test configuration, calibration curves can be derived which enable the unknown impulse to

be resolved. Extensive testing on all of the impulse balances has been conducted, such that the application of a variety of known impulses from the EFCS of different magnitudes and pulsewidths demonstrate the stability and repeatability of the measurements. The actual force produced by the EFCS was also independently calibrated by the microbalance method described by Selden and Ketsdever.[7] The error for a given applied force was found to be less than 2%. From these tests, a process has been developed to characterize the impulse balance well under any configuration.

A. Impulse Balance Model

The motion of the impulse balances can be described as an underdamped, harmonically oscillating system, and can be expressed in rotational or linear terms by the following:

$$I\ddot{\theta}(t) + C\dot{\theta}(t) + K\theta(t) = F(t)r = M(t) \tag{2}$$

$$I\ddot{x}(t) + C\dot{x}(t) + Kx(t) = F(t)r^2 = M(t)r$$

The angular solutions can easily be transformed into a linear deflection to correspond to the measurement methods used in the experimental setup. For the general case of forced motion of an underdamped system, consider $M(t) = M_o$ to be constant over a defined time period (pulse width) τ, as shown in Fig. 1b. This can be representative of either a constant impulse or steady-state situation, depending on the length of τ. The solution to Eq. (2) for initial conditions of angular displacement θ_o and angular velocity $\dot{\theta}_o$ is[10]

$$\theta(t) = \frac{M_o}{K} + e^{\alpha t}\left[\left\{\theta_o - \frac{M_o}{K}\right\}\cos\beta t + \left\{\frac{\dot{\theta}_o K - \alpha K\theta_o + \alpha M_o}{K\beta}\right\}\sin\beta t\right] \tag{3}$$

$$\dot{\theta}(t) = e^{\alpha t}\left[\dot{\theta}_o\cos\beta t + \left\{\frac{I\alpha\dot{\theta}_o - K\theta_o + M_o}{I\beta}\right\}\sin\beta t\right] \tag{4}$$

$$\ddot{\theta}(t) = e^{\alpha t}\left[\left\{\frac{M_o - C\dot{\theta}_o - K\theta_o}{I}\right\}\cos\beta t + \left\{\frac{\alpha\left(M_o - C\dot{\theta}_o - K\theta_o\right) - K\dot{\theta}_o}{I\beta}\right\}\sin\beta t\right] \tag{5}$$

where $\alpha = -C/2I = -\delta/T$ and $\beta = [K/I - \alpha^2]^{1/2}$. Note that by removing the damping term, the expected natural frequency $\omega_n = [K/I]^{1/2}$ for a simple torsional spring is obtained.

A closed-form analytical solution of the equation of motion in Eq. (2) is not possible for any arbitrary applied moment, M(t). However, the problem may be broken up into segments. Any arbitrary or irregular force can be reasonably approximated using a series of constant force segments of small time widths $d\tau$. The initial conditions of any given segment are simply the end state of the displacement and velocity terms from the previous segment. Equations (3-5) have been used to develop a simple software tool that has been validated using experimental data. The software has been used to examine the expected behavior of the NIBS for impulses of varying pulse widths and for steady state operations.

B. Signal Processing

The ability to obtain reliable and repeatable force measurements from NIBS depends on the time-varying deflection traces provided by the LVDT. The LVDT sensor provides an analog output, which commonly exhibits significant high frequency noise components. The noise can mostly be attributed to electrical sources (primarily in the 15Hz, 50Hz and 60Hz ranges). A number of signal analysis techniques have been used to perform denoising of the LVDT signal, including methods involving Fourier and wavelet transforms.[11,12] Both transform methods have been demonstrated to be quite reliable for deriving the total impulse from the deflection data. In either case, attention must be paid to not filter out more than just the noise from the signals.

III. Measurement Techniques

Once the raw data has been denoised through either the Fourier and/or wavelet transform methods, it can be analyzed using one or a combination of the following techniques:

a) In the simplest case, for $\tau \ll T$, the total impulse may be derived from the maximum deflection.
b) For τ on the order of T, the impulse must be examined by a time resolved impulse measurement technique.
c) For $\tau \gg T$, steady state analysis can be used.
d) Mass measurements can be made by taking advantage of the steady state analysis technique when the impulse balance is configured to rotate about a horizontal axis.

A. Maximum Deflection Analysis

Typically, impulse balances are operated using the assumption that the maximum deflection is linearly dependent on the delivered impulse.[3,4] The assumption is only strictly valid for laser pulsewidths (τ_i) much less than the natural period (T) of the balance. An analytical model was developed to examine the impulse balance characteristics. Figure 5 shows a comparison of the analytical model with experimental data demonstrating the maximum NIBS deflection as a function of τ_i / T for various total impulses. The dashed lines represent the theoretical fit using the experimentally derived thrust stand characteristics. As seen in Fig. 5 for $\tau_i > 0.1$ T, the direct correlation between the maximum balance displacement and the delivered impulse is no longer valid. For, $\tau_i \ll T$, the maximum deflection has a linear relationship with the total impulse. Figure 6 shows the NIBS maximum linear deflection as a function of applied impulse. The analytical model is in good agreement with the experimental data as shown in Fig. 6. The analytical model captures not only the trend of the experimental data, but is also in excellent agreement with the magnitude of the data.

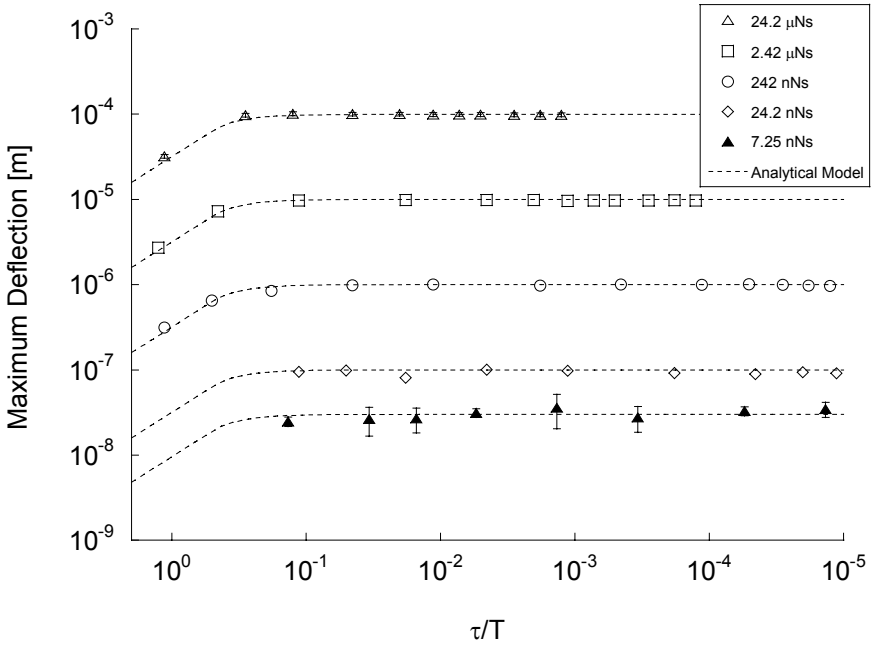

Figure 5. NIBS maximum deflection as a function of normalized impulse pulsewidth compared to the analytical model results. For $\tau \ll T$, the maximum deflection is constant. The data points represent experimental measurements with error bars showing the standard deviation of at least 10 repeated tests.

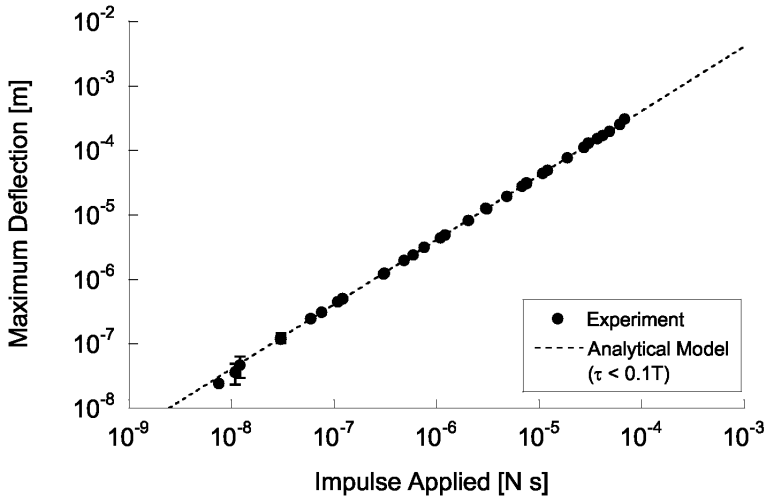

Figure 6. Comparison of maximum deflection versus applied impulse of the analytical model and experimental deflection data. Error bars represent the standard deviation of at least 10 repeated tests, and are typically smaller than the symbol used.

B. Time-Resolved Impulse Analysis

For larger τ_i, there are two possible scenarios. First, two different total impulses (say one with $\tau_i \ll T$ and one with $\tau_i \sim T$) can lead to the same maximum deflection; second, two identical total impulses with different pulsewidth can result in different maximum deflection. Therefore, another means by which to analyze the data is necessary if the pulsewidth is not known a priori. The Time-Resolved Impulse Measurement (TRIM) process is derived from Eq. (2). The equation of motion for the NIBS indicates that the force applied (as a function of time) is simply related to the addition of the position, velocity and acceleration components, which are scaled by the spring constant K, damping coefficient C, and the moment of inertia I, respectively as shown in Fig. 7.

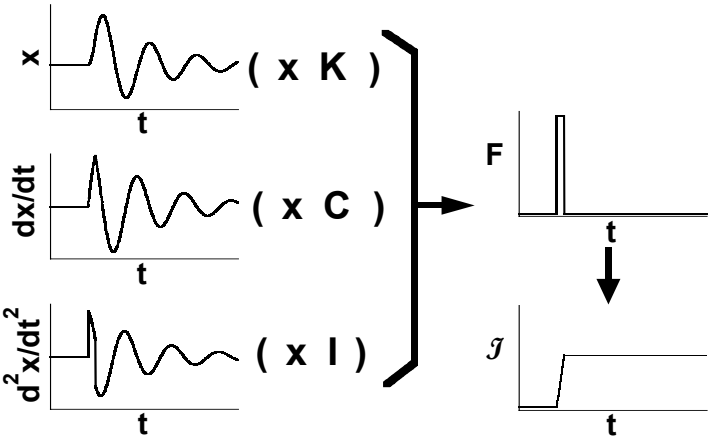

Figure 7. Schematic representation of the TRIM process for deriving the time-varying impulse or force from the balance's deflection and its derivatives.

Since the position (deflection) as a function of time is measured in the experiments, the derivative of the data must simply be taken once to obtain the velocity and twice for the acceleration. The major problem here is resolving the derivatives for a signal with noise. Using the signal processing methods previously described, the raw position data can be cleaned up significantly. In addition, a Savitzky-Golay algorithm is used to take the derivatives. This algorithm employs a moving window over which the points are fitted for a line. The slope of the line represents the

derivative of the point at the center of the window. This method results in artifacts at the beginning and end of a data trace. This method also tends to introduce slight aliasing effects, depending on the size of the window. However, it reliably maintains the content under the curve, which is essential for calculating the total impulse.

To complete the process, I, C and K need to be determined. The moment of inertia of the NIBS can be determined through a combination of physical measurement and CAD analysis. The spring constant and damping coefficient can then be determined from the position data by extracting the period of the oscillations T and the damping ratio δ, which is obtained from the natural logarithm of the ratio of successive peaks in the displacement data, $\delta = \ln[x_{max1}/x_{max2}]$. For completeness, it is also necessary to remember to include the term for the moment arm in Eq. (2). Finally, from the derived force F(t), the total impulse $\mathcal{I}(t)$ is given by integrating F(t).

C. Steady State Force Analysis

Forces are considered to be steady state when their durations are longer than the time the impulse balance requires to damp out motion. The measurements of such forces can be derived from the data by examining the net deflection of the balance after the oscillations have damped out and an equilibrium deflection has been reached. Figure 8 shows the difference between the deflections measured for impulsive (max. deflection) and steady state forces.

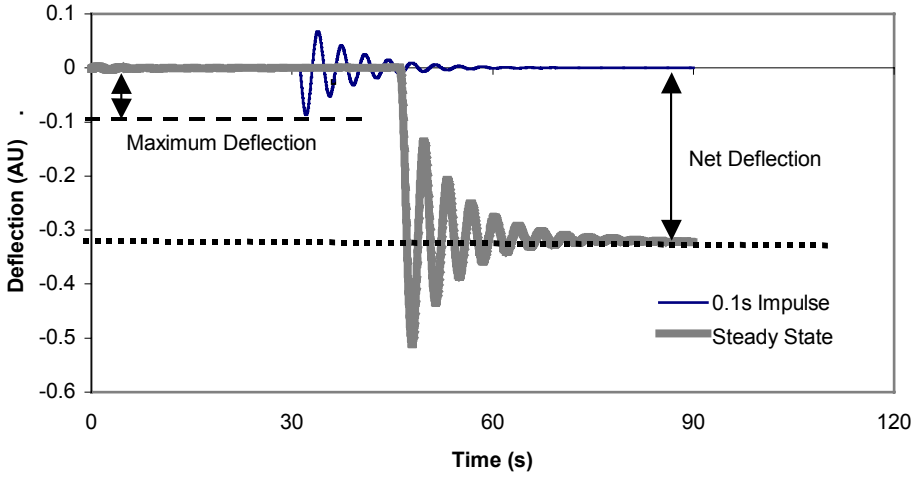

Figure 8. Comparison of deflection measurements for a 300μN force applied for 0.1s and steady state.

D. Mass Measurements

The full characterization of a thruster requires knowledge of both its impulse and its change in mass. When the impulse balance is configured in a manner similar to a traditional mass balance, a change in mass will result in the application of a steady state force equivalent to its weight. This steady state force will result in a net deflection. The deflection-to-mass relation can be derived using the EFCS. This measurement technique and experimental validation has been previously described by Pancotti et al.[9]

IV. Experimental Results

While it is important to verify the measurement techniques through modeling and simulation, nothing can replace test results from studying actual propulsion devices and other impulsive effects. As mentioned previously, there are a number of ongoing research studies which employ the impulse balances. An ongoing study with the NIBS system is the study of propulsive effects from laser-surface interactions such as vaporization and ablation. A parametric study is being conducted that varies the parameters such as the laser wavelength, pulse energy, spot size, and target material. In general, the laser pulsewidths are less than a few nanoseconds and the resulting ablation effects occur on similar timescales. Such timescales are much smaller than the natural period of the stand, and allow for simple deflection analysis to be used. It is not possible to time resolve these forces, as time response limitations

due to electronic hardware becoming an overwhelming source of noise in the system. Figure 9 demonstrates a typical set of results required to resolve the total impulse for such ablation effects. The trace on the right is of the impulse from a 1064nm laser on Delrin polymer. Based on the calibration curve (on the left) derived using the EFCS data taken before and after the laser test, an equation can be derived that relates the maximum deflection voltage read by the LVDT to a known impulse. Using the curve presented in Fig. 9, a total impulse of approximately 15 micro-Newton-seconds can be calculated. It is important to note that although very quick ablation effects typically dominate, slower and longer impulse generating processes may also occur. In these cases it is necessary to also employ the time-resolved method to gain further insight into the laser-surface interactions. In particular, interactions with polymers such as Teflon and Delrin at very low fluences have demonstrated that other heating mechanisms may be as significant and dominate the ablation processes.

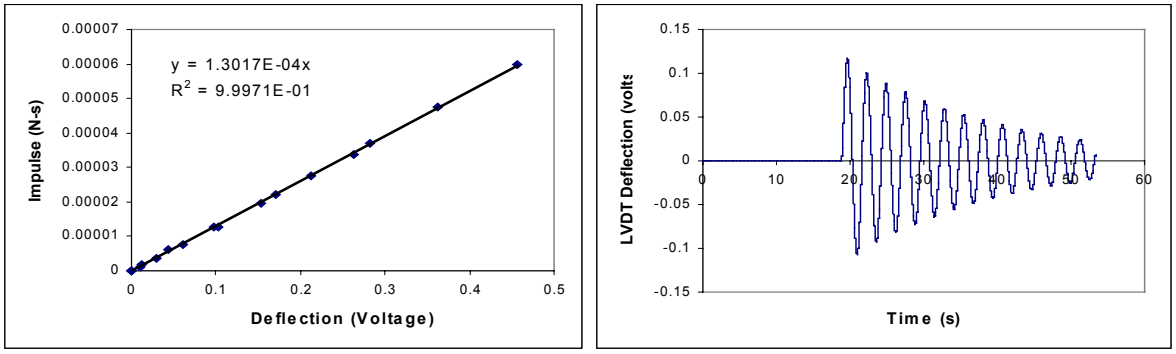

Figure 9. A typical calibration curve (left) allows for maximum deflection analysis to be used on most laser ablation traces (right), since the ablation mechanisms generally occur on timescales on the order of microseconds or less. Deflection analysis will show that this trace corresponds to an impulse of approximately 15 micro-Newton-seconds.

Another set of testing is being done with a number of Tanner Research Inc. MEMS-based solid-propellant motors. Solid propellant is packed into a small channel and is ignited using an electrical charge. These microthrusters are being designed to be single use and give a single impulse bit of known magnitude. The design of these devices is constantly evolving. The impulse balances are used to examine the total impulse generated by many different design configurations. From these impulse measurements, more efficient designs are being developed. In general, these tests are being conducted using the maximum deflection method. However, a number of the traces have exhibited peculiarities or special characteristics that can further be explored using the TRIM process to obtain time-resolved force profiles. Figure 10 is an example of a microthruster designed to have slow burning characteristics. The TRIM process can time resolve the performance of such a thruster. After performing the TRIM process on the data, the impulse had a duration of approximately 0.7s (FWHM), which was on the order of the natural period of the stand. It was also clear that the force generated was not constant. Two peaks in the force are evident. Such information can help to discover flaws or problems in the design of the thruster.

As this study of the Tanner digital microthrusters progressed, the designs have evolved to the point where examining the change in mass due to the combustion reaction is also of great benefit. The solid-propellant microthrusters continued to be studied using the TSMB. Figure 11 shows the test results using a combination of the TRIM process and mass measurement technique for a rapid impulse microthruster design. These thrusters would typically result in traces similar to the ablation tests depicted in Fig. 9. The deflection trace in Fig. 11 shows an anomaly that the resulting motion is stimulated by an impulse on the order of the natural period of the balance. In this case the experiment was setup to give a negative deflection. As expected, there is a net deflection as the impulse balance damps to a rest state. The TRIM process reveals that the impulse generated by the thruster was not uniform, as two sharp peaks are clearly present. Ideally, these microthrusters should give a single and consistent impulse. Most of the thrusters in this batch of testing did deliver a single, rapid impulse bit as expected. This particular thruster exhibited an anomalous force profile. The ability to detect such anomalies could reveal manufacturing inconsistencies and provide insight into possible design and performance issues. Repeated testing of such a microthruster design could lead to better understanding of the impulsive mechanisms and ultimately a better design. Again it is important to note that calibration is an important part of such testing. Calibration sets taken before and after the thruster firings are collected using the EFCS. By applying a series of known impulse and steady state forces, in the test configuration, the motion of the impulse balance can be well characterized. Using this

information allows the voltage readings provided by the LVDT to be transformed using the TRIM process and scaled to known force levels. For the thruster presented in Fig. 11, the resulting change in mass was found to be 4.58 mg +/- 2%.

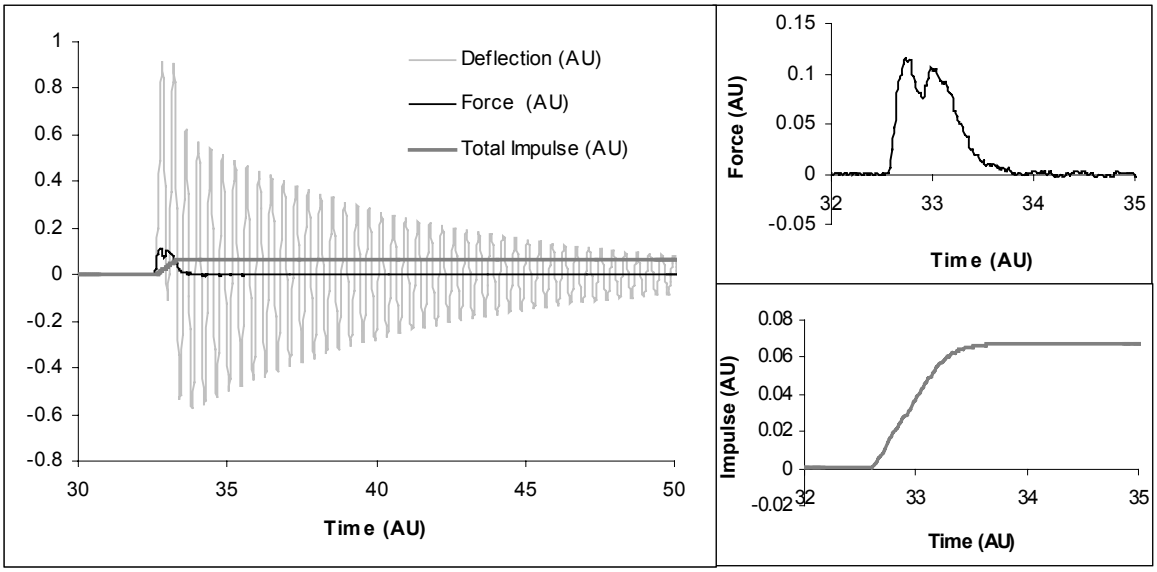

Figure 10. Example of time resolved force and total impulse measurements from the deflection data for a slow-burning Tanner digital microthruster. The panels on the right side show a magnified section of the force (top) and total impulse (bottom) curves.

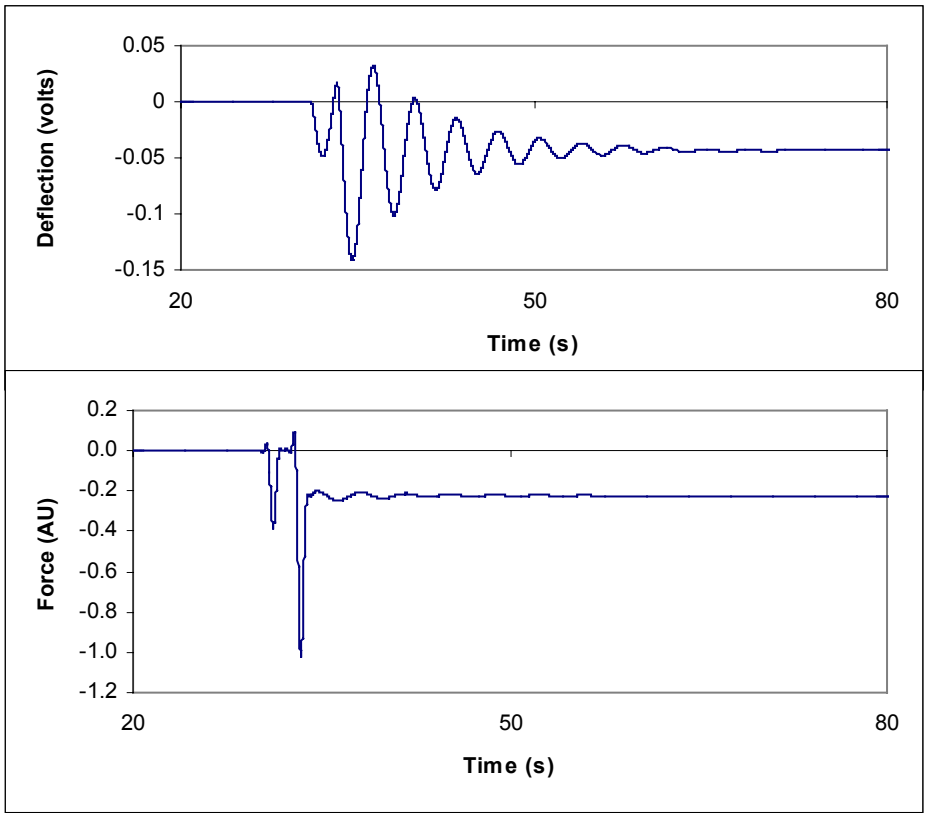

Figure 11. Time resolved force profile for a Tanner digital microthruster using the TSMB configuration to resolve change in mass. The steady state force component at the end of the trace represents the resulting force corresponding to a change in mass.

V. Conclusions

The many versions of the impulse balance have proven to be highly reliable and accurate as a diagnostic tool for the research of impulsive forces from micropropulsion devices and other physical phenomena. The impulse balance has also proven to be highly adaptable to handle many different configurations. The impulse balances have been made to operate in air or vacuum, under heavy or light loads, using electrical and even gas connections to the targets. The simplicity of the balance systems allowed for detailed modeling and characterization of the systems and the development of robust analytical processes.

Depending on the requirements of the test, the impulse balances can provide simple total impulse analysis through measurement of the maximum deflection. It can just as easily be adapted to provide time-resolved force measurements for impulsive forces. The TRIM process allows for the time resolution of forces ranging from steady state to rapid and repeated impulses. The extension of operating conditions of impulse balances to arbitrary impulse pulsewidth, shape, and magnitude (down to 7 nNs) has been demonstrated with the NIBS using a combination of an analytical code and a data analysis method. And the recent addition of magnetic damping techniques and mass measurement provide a necessary toolset for a robust impulse measurement system.

Previous studies[3,4] have been limited to data analysis based on the assumption that $\tau \ll T$. For basic research involving new propulsion systems and photon-surface interactions, the characteristic time-dependence of the impulse of a particular process may not be known a priori, making a generalized scheme necessary to time-resolve the impulse delivery to the balance. Also, a torsional impulse balance can deflect the same amount for different total impulses (e.g. see Fig. 5), particularly where the assumption of $\tau \ll T$ is no longer valid. Under similar pulsewidth conditions, an impulse balance can also deflect differently for equivalent total impulses. Therefore, a generalized τ-independent data analysis tool is required.

The NIBS has already demonstrated that it can be used to time-resolve impulses. The real issues now become that of performance. The common measure of an impulse balance's performance is typically that of impulse magnitude resolution. The NIBS has repeatedly measured impulses as low as 7nNs and as high as hundreds of micro-Newton-seconds, and has consistently derived results that fall within 4.5% (worst case) of the applied impulse. However, when time resolving the forces, it becomes apparent that there are more performance related issues than just the magnitude of the impulse. Qualitatively, the accuracy of the shape of the time-varying force is of interest. In other words, how closely the derived force matches the applied force over time is important in determining the overall effectiveness of both the TRIM technique and the NIBS itself. Noise and time response of the whole system then become significant issues.

Noise in the measured signal from the NIBS is one of the largest sources of error in the TRIM process. Excessive noise affects the derivatives of the deflection trace and results in noisy time-resolved forces or impulses. There are several sources of noise including external physical vibrations, temperature variations, and electronic noise directly from the LVDT and its signal conditioner. The simplest way to eliminate a significant portion of the electronic noise is the use of a well-tuned low-pass filter (LPF). The impulse balance itself must be considered for time response issues. The NIBS has been extensively tested with calibration impulses of pulsewidth τ as low as 10^{-7} sec up to minutes in length. The NIBS has also repeatedly provided excellent results for examining laser ablation effects, which occur on the order of nanoseconds. The main time response limitations have been attributed to the LVDT and its signal conditioner. The TRIM process only currently provides accurate results for pulsewidths as low as 0.05 seconds due to aliasing. Improvement of the techniques described here would be easily achieved through improvements of the overall hardware system time response.

Ultimately, the performance of the impulse balance comes down to repeatability. For the maximum deflection analysis, the experimental error was taken as the standard deviation of between five and ten data points and was typically less than ±2% (i.e. smaller than the symbol size in Figs. 7 and 8 unless otherwise indicated). For the time-resolved impulse analysis, all derivations of total impulse from the deflection measurements have resulted in errors less than ±4.5%, which encapsulates all sources of error including from the applied force.

The repeatability of the data from each of the impulse balances suggests that it is a viable diagnostic tool for the investigation of arbitrarily produced impulses from a variety of devices and physical phenomena. Considering the advantages and limitations of the NIBS, there are a number of new innovative micropropulsion devices and laser-surface interactions that could be investigated with benefit from the direct measurement of the impulsive forces.

Acknowledgments

This work was supported by the Air Force Research Laboratory, Propulsion Directorate, Space and Missile Propulsion Division (AFRL/PRSA), Edwards AFB, California. The MEMS-based digital microthrusters were

provided by Dr. Amish Desai of Tanner Research, Inc. Additional experimental testing was performed by Nathaniel Selden and Anthony Pancotti (USC). One of the authors (BD) was also supported in part by a graduate assistantship from the Department of Aerospace and Mechanical Engineering and the Astronautics and Space Technology Division at the University of Southern California.

References

[1] R.G. Jahn, *Physics of Electric Propulsion,* McGraw-Hill, New York, 1968.

[2] G. Spanjers, K. McFall, F. Gulczinski, and R. Spores, "Investigation of propellant inefficiencies in a pulsed plasma thruster," *AIAA Paper No. 1996-2723, 32nd Joint Propulsion Conference,* 1996.

[3] E. Cubbin, J. Ziemer, E. Choueiri, R. Jahn, "Pulsed thrust measurements using laser interferometry," *Rev. Sci. Instrum.* Vol. 68, No.6, 1997, pp.2339-2346.

[4] M. Gamero-Castano, "A torsional balance for the characterization of microNewton thrusters," *Rev. Sci. Instrum.* Vol.74, No.10, 2003, pp. 4509-4514.

[5] T. Haag, "Thrust stand for pulsed plasma thrusters," *Rev. Sci. Instrum.* Vol. 68, No.5, 1997, pp. 2060-2067.

[6] A. Jamison, A. Ketsdever, and E.P. Muntz, "Gas dynamic calibration of a nano-Newton thrust stand," *Rev. Sci. Instrum.* Vol. 73, No.10, 2002, pp. 3629-3637.

[7] N. Selden and A. Ketsdever, "Comparison of force balance calibration techniques for the nano-Newton range," *Rev. Sci. Instrum.* Vol. 74, No.12, 2003, pp. 5249-5254.

[8] B.D'Souza, A.D.Ketsdever, "Investigation of time-dependent forces on a nano-Newton-second impulse balance", Rev.Sci. Instrum., Vol. 76, No.1, 2005, pp.015105 1-10

[9] A.P.Pancotti,A.D.Ketsdever, V.Aguero, J.Watjen, P.R.Schwoebel, "Development of a Thrust Stand Micro-Balance to Assess Micropropulsion Performance," *AIAA Paper No. 2005-4415, 41st Joint Propulsion Conference,* 2005.

[10] R.K. Vierck, *Vibration Analysis,* Thomas Y. Crowell, New York, 1979.

[11] C. Gasquet and P. Witomski, *Fourier Analysis and Applications: Filtering, Numerical Computation, Wavelets,* Springer-Verlag, NewYork, 1999.

[12] L.M Jameson, *Wavelets Theory and Applications,* edited by G. Erlebacher, M.Y. Hussaini, and L.M.Jameson, Oxford University Press, New York, 1996, pp. 1-37.